

# Enhanced Activity and Stability of TiO<sub>2</sub>-Coated Cobalt/Carbon Catalysts for Electrochemical Water Oxidation

Hyung Ju Kim,<sup>†,||</sup> David H. K. Jackson,<sup>‡</sup> Jechan Lee,<sup>†</sup> Yingxin Guan,<sup>§</sup> Thomas F. Kuech,<sup>†,‡,§</sup> and George W. Huber<sup>\*,†</sup>

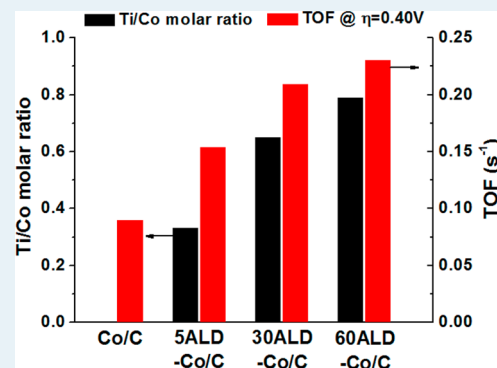
<sup>†</sup>Department of Chemical and Biological Engineering, University of Wisconsin-Madison, 1415 Engineering Drive, Madison, Wisconsin 53706, United States

<sup>‡</sup>Materials Science Program, University of Wisconsin-Madison, 1509 University Avenue, Madison, Wisconsin 53706, United States

<sup>§</sup>Department of Materials Science and Engineering, University of Wisconsin-Madison, 1509 University Avenue, Madison, Wisconsin 53706, United States

## S Supporting Information

**ABSTRACT:** TiO<sub>2</sub>-coated Co/C catalysts prepared by atomic layer deposition (ALD) were used to study the effect of TiO<sub>2</sub> overcoating on a Co/C catalyst for electrochemical water oxidation. The Co/C catalyst with a thin-layer overcoating of TiO<sub>2</sub> (ALD(TiO<sub>2</sub>)-Co/C) demonstrated 2.5 times higher turnover frequency (TOF) than the Co/C catalyst for the reaction. The TOF of the ALD(TiO<sub>2</sub>)-Co/C catalyst increased when the ALD(TiO<sub>2</sub>) coating cycle number was increased from 5 to 60. In addition, the stability of the 60 cycle ALD(TiO<sub>2</sub>)-Co/C catalyst was enhanced compared to the Co/C catalyst. This work shows how the ALD synthesis technique can be used to improve the catalytic activity and stability of nonprecious-metal-based catalysts like Co/C for electrochemical water oxidation.



**KEYWORDS:** water oxidation, Co catalyst, atomic layer deposition, TiO<sub>2</sub> coating, Co–TiO<sub>2</sub> interface

Water electrolysis ( $2\text{H}_2\text{O} \rightarrow 2\text{H}_2 + \text{O}_2$ ) is an important industrial reaction to produce hydrogen and oxygen.<sup>1–3</sup> The produced hydrogen can be used for removing oxygen from biomass,<sup>4–7</sup> powering fuel cells,<sup>8–10</sup> or hydrotreating in the petrochemical industry.<sup>11</sup> For water electrolysis, water oxidation for oxygen evolution at the anode ( $4\text{OH}^- \rightarrow \text{O}_2 + 2\text{H}_2\text{O} + 4\text{e}^-$  at high pH) has been recognized as more critical compared to the hydrogen evolution reaction at the cathode ( $4\text{H}_2\text{O} + 4\text{e}^- \rightarrow 2\text{H}_2 + 4\text{OH}^-$  at high pH) because it requires a higher overpotential.<sup>1,2,12</sup> Pt has been commonly used as a catalyst for electrochemical reactions because of its high activity and stability.<sup>1,2</sup> However, it has high cost and limited availability. Metal oxide materials have been tried as Pt replacements, because they are abundant and cheap. RuO<sub>2</sub> and IrO<sub>2</sub> have been reported as active electrocatalysts for water oxidation in acid condition.<sup>13,14</sup> However, these metal oxides are still expensive and not earth-abundant. Researchers have tried to develop nonprecious-metal-based catalysts using cost-effective and abundant materials such as cobalt or nickel, which reduce the necessary overpotential and increase activity for the water oxidation reaction in alkaline condition.<sup>15–31</sup> However, substantial progress is still required to enhance the activity and stability of nonprecious metal catalysts.

Atomic layer deposition (ALD) is a technique that allows the growth of conformal thin coatings through a self-limiting vapor growth process.<sup>32,33</sup> This technique can be used to prepare new

types of atomically controlled catalysts.<sup>34–38</sup> Previous studies have shown that ALD of a metal oxide (e.g., Al<sub>2</sub>O<sub>3</sub> or TiO<sub>2</sub>) overcoat can inhibit leaching of base metal nanoparticles such as Cu or Co.<sup>35,36</sup> In addition, the ALD technique can be used to synthesize novel bifunctional catalysts by the addition of an acidic oxide layer to the stabilizing overcoat for liquid-phase hydrogenation reactions.<sup>37,38</sup> It has also been reported that the overcoat of metal oxides by ALD can stabilize semiconductor photoelectrodes and increase performance in photoelectrochemical applications.<sup>39–43</sup>

Here we report that thin TiO<sub>2</sub> coating by ALD can be used to increase catalytic activity and stability of carbon-supported cobalt catalysts (Co/C) for electrochemical water oxidation. We first prepared the Co/C catalyst by incipient wetness impregnation and then synthesized an ALD titania (TiO<sub>2</sub>)-coated Co/C catalyst (ALD(TiO<sub>2</sub>)-Co/C) to investigate the effect of the TiO<sub>2</sub> overcoat on the Co/C catalyst (see Figure S1 and Supporting Information). As we will demonstrate in this paper, the prepared ALD(TiO<sub>2</sub>)-Co/C shows 2.5 times higher catalytic activity than the commercial Pt/C catalyst for the water oxidation reaction. The activity of ALD(TiO<sub>2</sub>)-Co/C catalyst increases with increasing Ti/Co molar ratio (and

Received: January 27, 2015

Revised: April 30, 2015

Published: May 4, 2015

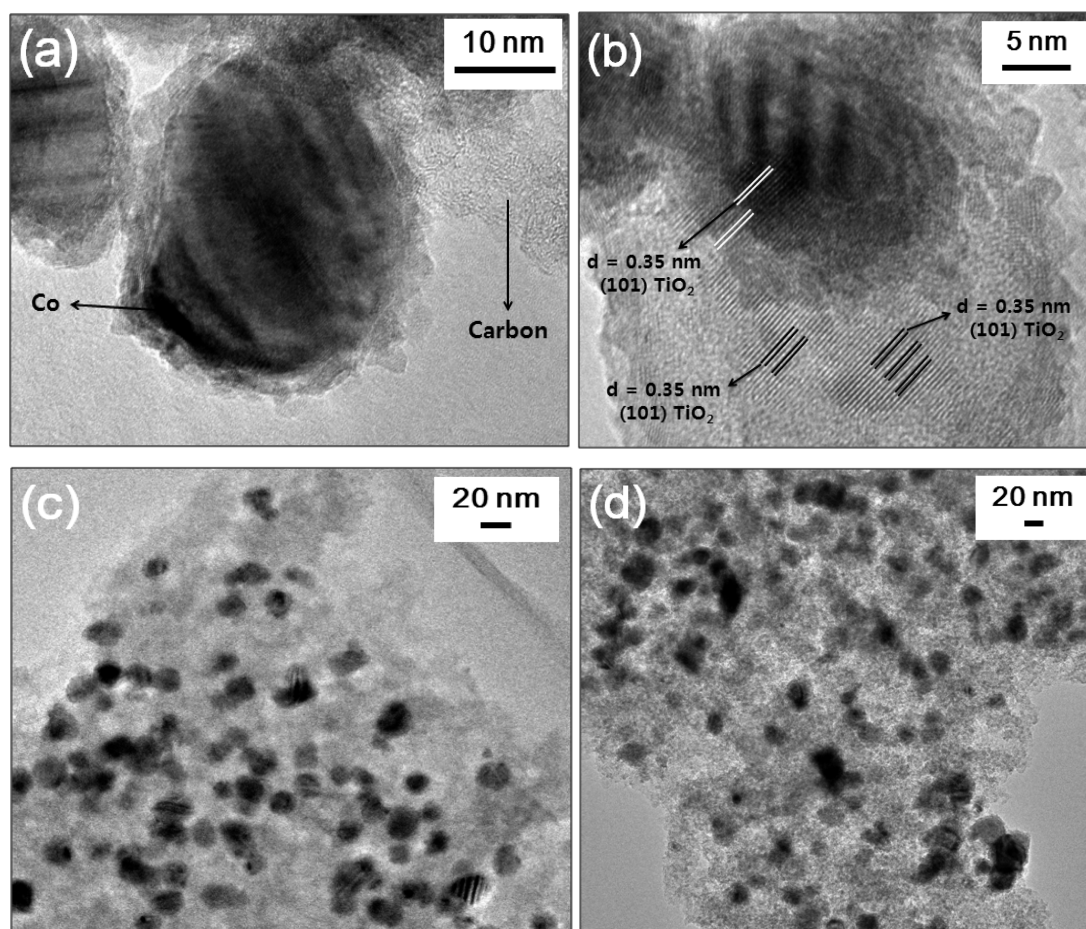


**Figure 1.** Structural characterization of ALD(TiO<sub>2</sub>)-Co/C catalysts. (a) High-resolution TEM image of 5 cycle ALD(TiO<sub>2</sub>)-Co/C catalytic system. (b) High-resolution TEM image of 5 cycle ALD(TiO<sub>2</sub>)-Co/C catalyst with interplanar distance measurement of TiO<sub>2</sub>. (c) TEM image of 30 cycle ALD(TiO<sub>2</sub>)-Co/C catalyst. (d) TEM image of 60 cycle ALD(TiO<sub>2</sub>)-Co/C catalyst.

increasing ALD coating cycles). Also, the stability of the ALD(TiO<sub>2</sub>)-Co/C catalyst is enhanced (only ~25% activity loss after 8 h) compared to the Co/C catalyst (~50% activity loss after 8 h).

Figure 1a–d exhibit representative high-resolution transmission electron microscope (HR-TEM) images for structural characterization of prepared ALD(TiO<sub>2</sub>)-Co/C catalysts. Mean particle size of the catalysts were calculated from observation of over 120 particles in the TEM images. As shown in Table 1, the prepared Co/C and ALD(TiO<sub>2</sub>)-Co/C catalysts have Co particles of 20 ± 7 nm size that are distributed on conventional carbon support. In the X-ray diffraction (XRD) pattern of as-prepared Co/C (Figure S2), hexagonal close-packed (HCP) Co could be detected as the predominant phase. Peaks indicating the formation of this phase can be seen at 44.73° and 47.63°, corresponding to crystal planes of (002) and (101), respectively.<sup>44,45</sup> Both the XRD pattern (Figure S2) and the interplanar spacing (Figure 1b) of the ALD(TiO<sub>2</sub>)-Co/C catalyst indicate that anatase is the predominant TiO<sub>2</sub> phase. Figure 1a also shows that the synthesized catalyst has a surface oxide layer with 2–3 nm thickness on Co metal. The TiO<sub>2</sub> forms a thin film over the cobalt particle during the ALD process. After calcination, the TiO<sub>2</sub> forms pores. In the TiO<sub>2</sub>-coated Co/C catalyst, the thin TiO<sub>2</sub> film probably decorates the under-coordinated cobalt sites located at defects, corners, and edges which thereby prevents the sintering or leaching of cobalt.<sup>36</sup> The decoration of the Co with TiO<sub>2</sub> is shown in

Figure 1b in the TEM images. This figure shows that the TiO<sub>2</sub> can deposit on both the carbon and the Co particles.

The ALD(TiO<sub>2</sub>)-Co/C catalysts were studied for electrocatalytic water oxidation in an electrochemical cell having three electrodes at room temperature in an aqueous 1 M KOH solution. In Figures 2, 3, S3 and S4, the catalytic activity of the Co/C and ALD(TiO<sub>2</sub>)-Co/C catalysts were examined by linear sweep voltammetry (LSV) for electrocatalytic water oxidation. The scan potential was from 0 to 0.9 V (vs Hg/HgO) at a scan rate of 5 mV s<sup>-1</sup>. It is noteworthy that the total catalyst amount loaded on the glassy carbon working electrode (area: ca. 0.07 cm<sup>2</sup>) was 0.916 mg/cm<sup>2</sup> for all the catalysts tested, but the Co loading for the ALD(TiO<sub>2</sub>)-Co/C catalysts decreased with the number of ALD cycles because of titania overcoat mass gain (see Figure S5 and Table 1). The catalytic performances of all catalysts examined in this study were evaluated in terms of the following five aspects: (1) overpotential ( $\eta$ ) = applied potential – thermodynamic potential, (2) current divided by geometric electrode area ( $i_{\text{geo}}$ ), (3) current divided by entire surface area of the carbon support that was deposited on the glassy carbon electrode ( $i_{\text{support}}$ ), (4) current divided by Co metal loading ( $i_{\text{mass}}$ ), and (5) turnover frequency (TOF), defined as current divided by the number of sites, which was determined on the basis of metal dispersion estimated by TEM analysis (see Figure S6 and Table S1 in Supporting Information). The electrocatalytic performance results were summarized in Table 1. In Figure 2 a,b, only the ALD TiO<sub>2</sub> overcoat on the carbon

Table 1. Electrocatalytic Activity Data for Water Oxidation at Room Temperature and in an Aqueous 1 M KOH Solution

catalyst system	cobalt loading (Ti/Co mol ratio) [mg/cm <sup>2</sup> ]	size <sup>a</sup> [nm]	$\eta$ at 10 mA/cm <sup>2</sup> [mV]	$i_{\text{geo}}^c$ at $\eta = 0.40, 0.38$ V [mA/cm <sup>2</sup> ]	$i_{\text{support}}^d$ at $\eta = 0.40, 0.38$ V [ $\mu$ A/cm <sup>2</sup> ]	$i_{\text{mass}}^e$ at $\eta = 0.40, 0.38$ V [A/g]	TOF <sup>f</sup> at $\eta = 0.40, 0.38$ V [s <sup>-1</sup> ]
05ALD(TiO <sub>2</sub> )-Co/C	0.144 (0.33)	20.4 ± 5.3	411	8.6 (0.40 V) 6.4 (0.38 V)	1.84 (0.40 V) 1.37 (0.38 V)	59.9 (0.40 V) 44.6 (0.38 V)	0.154 (0.40 V) 0.114 (0.38 V)
30ALD(TiO <sub>2</sub> )-Co/C	0.120 (0.65)	21.0 ± 7.9	402	9.5 (0.40 V) 6.3 (0.38 V)	2.44 (0.40 V) 1.62 (0.38 V)	79.4 (0.40 V) 52.7 (0.38 V)	0.209 (0.40 V) 0.139 (0.38 V)
60ALD(TiO <sub>2</sub> )-Co/C	0.112 (0.79)	20.3 ± 7.7	398	10.1 (0.40 V) 6.8 (0.38 V)	2.79 (0.40 V) 1.89 (0.38 V)	90.2 (0.40 V) 61.1 (0.38 V)	0.230 (0.40 V) 0.156 (0.38 V)

<sup>a</sup>Mean particle size calculated from observation of 120 particles in the TEM images. <sup>b</sup> $\eta$  (overpotential) = applied potential – thermodynamic potential. <sup>c</sup> $i_{\text{geo}}$  = current divided by geometric electrode area (glassy carbon: 0.07 cm<sup>2</sup>). <sup>d</sup> $i_{\text{support}}$  = current divided by the glassy carbon electrode. <sup>e</sup> $i_{\text{mass}}$  = current divided by Co metal loading (g). <sup>f</sup>TOF = turnover frequency for oxygen evolution assuming that every Co surface atom is catalytically active and Faradaic efficiency is 100%, which refer to the rate of electron delivery per surface cobalt atom per second.

support had very low activity in terms of  $i_{\text{geo}}$  at  $\eta = 0.4$  V and  $\eta$  at  $i_{\text{geo}} = 10$  mA/cm<sup>2</sup> compared to the Co/C catalyst. This could be expected from previous literature demonstrating that TiO<sub>2</sub> binds O and OH weakly, which is a characteristic associated with low water oxidation activity.<sup>13</sup> However, the Co/C catalyst with an overcoating of TiO<sub>2</sub> demonstrated higher  $i_{\text{geo}}$  at  $\eta = 0.4$  V (also 2 times higher  $i_{\text{mass}}$ ) and lower  $\eta$  at  $i_{\text{geo}} = 10$  mA/cm<sup>2</sup> than the Co/C catalyst for the reaction. This result suggests that interactions between Co and TiO<sub>2</sub> in the TiO<sub>2</sub> coated Co/C catalyst leads to improved catalytic activity. In Figure 3 and Table 1, the catalytic performances of ALD(TiO<sub>2</sub>)-Co/C catalysts increased with increasing ALD(TiO<sub>2</sub>) coating cycle number from 5 to 60. The  $\eta$  of water oxidation for ALD(TiO<sub>2</sub>)-Co/C catalysts had lower values than the Co/C catalyst. As shown in Figure 3a and S4, the  $i_{\text{geo}}$ ,  $i_{\text{support}}$  and  $i_{\text{mass}}$  (at  $\eta = 0.38, 0.4$  V) of the ALD(TiO<sub>2</sub>)-Co/C catalysts toward electrocatalytic water oxidation decreased in the following order: 60 cycle ALD(TiO<sub>2</sub>)-Co/C > 30 cycle ALD(TiO<sub>2</sub>)-Co/C > 5 cycle ALD(TiO<sub>2</sub>)-Co/C. The  $i_{\text{mass}}$  of water oxidation on 60 cycle ALD(TiO<sub>2</sub>)-Co/C was 2.32 times higher than that of the Co/C catalyst. Figure 3b shows changes of Ti/Co molar ratio and TOF according to ALD coating cycle. As shown in Figure 3b, the TOFs of ALD(TiO<sub>2</sub>)-Co/C catalysts also increased with increasing Ti/Co molar ratio (and increasing ALD coating cycles). Figure 3c shows Tafel plots of Co/C and ALD(TiO<sub>2</sub>)-Co/C catalysts. Figure 3d shows the change of Tafel slopes with Ti/Co molar ratio (different ALD coating cycles). For the uncoated Co/C catalyst, a Tafel slope of 169 mV/dec was calculated from the overpotential ( $\eta$ ) – log  $i$  (A/cm<sup>2</sup>) plots, which agrees with the values calculated from the previous experiments with cobalt electrodes.<sup>46,47</sup> The Tafel slopes for ALD(TiO<sub>2</sub>)-Co/C catalysts decreased with increasing Ti/Co ratios. The Tafel slope at the highest Ti/Co ratio was similar to the reported Tafel slope (122 mV/dec) for an aged Co electrode that was surface-oxidized by an electrochemical treatment.<sup>47</sup> The 60 cycle ALD(TiO<sub>2</sub>)-Co/C had the lower Tafel slope, largest  $i_{\text{mass}}$  and higher TOF among the tested catalysts.

XPS analysis was conducted to elucidate the surface species present on the synthesized catalysts. Figure 4 shows the Co(2p) and Ti(2p) regions in the XPS spectra of Co/C and ALD(TiO<sub>2</sub>)-Co/C catalysts. In the as-made Co/C catalyst, Co 2p<sub>3/2</sub> peak has a binding energy (BE) of 780.7 eV, which is attributed to Co(OH)<sub>2</sub> species.<sup>48,49</sup> The BE (781.3 eV) of Co 2p<sub>3/2</sub> peak in the ALD(TiO<sub>2</sub>)-Co/C catalysts is higher than that of the Co 2p<sub>3/2</sub> peak in the Co/C catalyst and is similar to that observed in Co doped (5%) in TiO<sub>2</sub> (781.5 eV).<sup>50</sup> In addition, the Co 2p<sub>3/2</sub> region has two components, a primary peak denoted as Co  $\alpha$  and a satellite peak denoted as Co  $\beta$ . The area ratio of Co  $\alpha$  area/Co  $\beta$  area decreased with increasing Co loading on TiO<sub>2</sub> caused by interaction between Co and TiO<sub>2</sub>.<sup>50</sup> This ratio also decreased as the TiO<sub>2</sub> loading increased for the ALD(TiO<sub>2</sub>)-Co/C catalysts. The Co  $\alpha$  peak at 781.3 eV in the ALD(TiO<sub>2</sub>)-Co/C catalysts has also been attributed to Co<sup>2+</sup> in the Co–O–Ti phase.<sup>51</sup> The Co  $\alpha$  peak at 781.3 eV has a BE lower than that of Co<sup>2+</sup> in a CoO phase.<sup>51</sup> This can be explained by the weakening of the Co–O bond because of the formation of Co–O–Ti configuration.<sup>51</sup> It has been reported that the rate-limiting step in water oxidation is the reaction of an adsorbed OH<sup>-</sup> anion with an adsorbed O atom to form OOH species.<sup>13,18,20,52</sup> The catalytic water oxidation activity can be increased by modifying the BE of O or OH species on the surface.<sup>13,52–54</sup> The formation of Co–O–Ti configuration



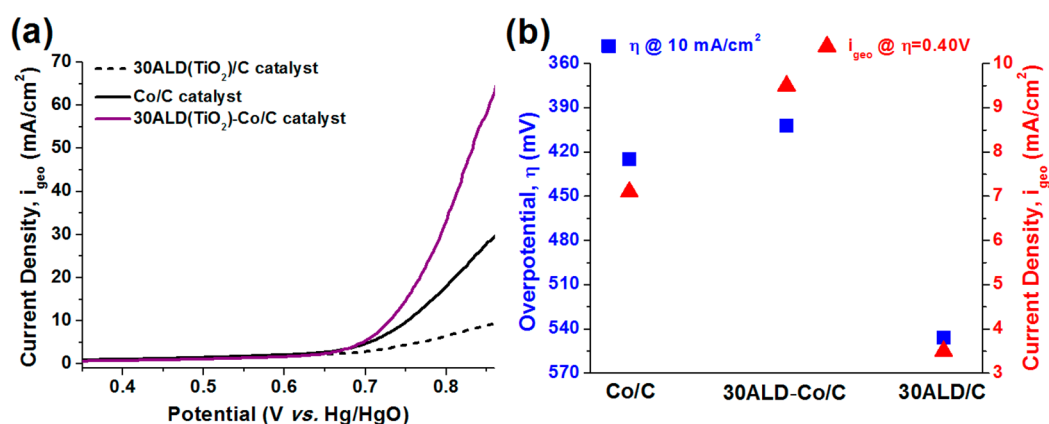


**Figure 2.** Electrocatalytic water oxidation activity of Co/C and ALD(TiO<sub>2</sub>)-Co/C catalysts at room temperature and in an aqueous 1 M KOH solution. (a) LSV curves of Co/C, 30 cycle ALD(TiO<sub>2</sub>)/C and 30 cycle ALD(TiO<sub>2</sub>)-Co/C. (b) Comparisons of required overpotential ( $\eta$ ) at 10 mA/cm<sup>2</sup> and current divided by geometric electrode area at  $\eta = 0.4$  V for Co/C, 30 cycle ALD(TiO<sub>2</sub>)/C and 30 cycle ALD(TiO<sub>2</sub>)-Co/C.

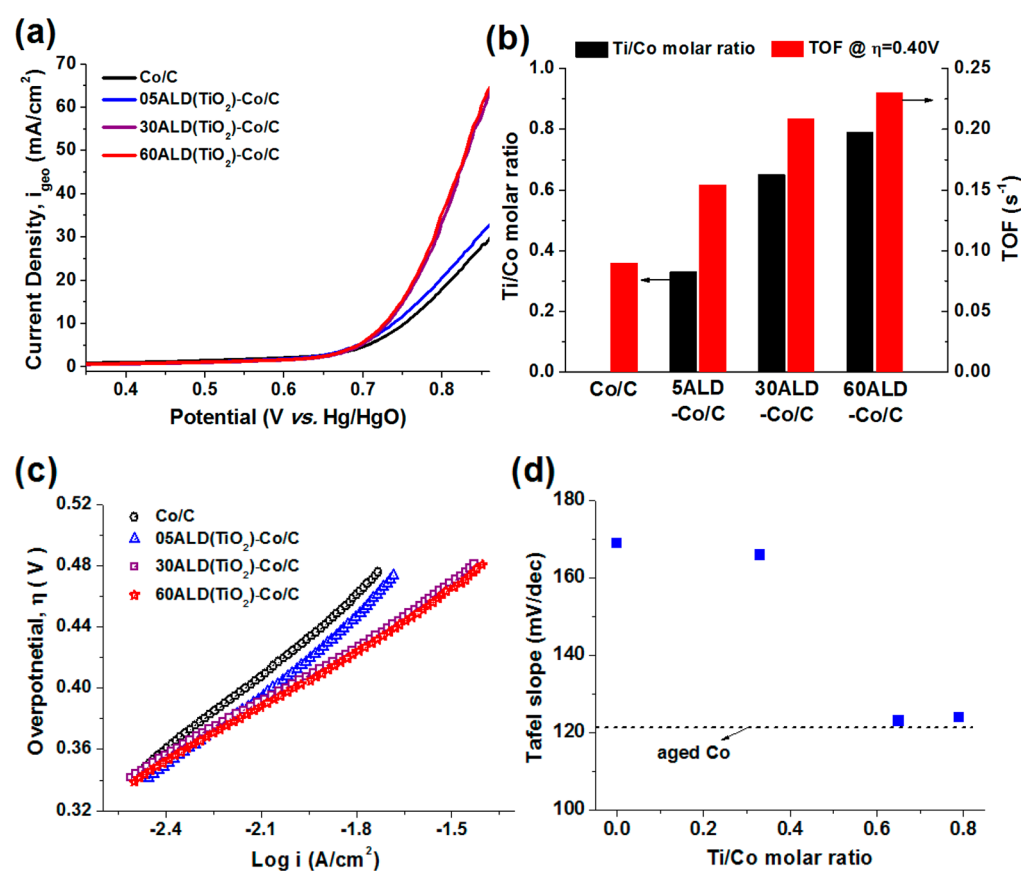


**Figure 3.** Effect of ALD coating cycle number on ALD(TiO<sub>2</sub>)-Co/C for electrocatalytic water oxidation. (a) LSV curves of ALD(TiO<sub>2</sub>)-Co/C with different ALD coating cycle number. (b) Changes of Ti/Co molar ratio and TOF according to ALD coating cycle number. (c) Tafel plots of Co/C and ALD(TiO<sub>2</sub>)-Co/C catalysts. (d) Change of Tafel slopes with Ti/Co molar ratio. Dashed line indicates a Tafel slope of 122 mV/dec for aged Co electrode (surface oxidized Co by an electrochemical treatment) and are shown for reference.

mediated by the interaction between Co and TiO<sub>2</sub> may change the surface BE of O or OH species on the catalyst, thereby facilitating the formation of O–OH, which could enhance the water oxidation activity. The Co BE of TiO<sub>2</sub> overcoated Co/C catalysts shifts to higher BE as the ALD(TiO<sub>2</sub>) cycle number increases, reflecting enhanced oxidation of the surface Co oxide by TiO<sub>2</sub> coating.<sup>49</sup> The large observed peak widths of Co  $\beta$  with increasing TiO<sub>2</sub> coating suggests that other species, such as Co(III) or Co(IV), may be present on our catalysts samples. Co<sub>3</sub>O<sub>4</sub> is more active than CoO for the oxygen evolution

reaction.<sup>17</sup> It is also known that the activity of cobalt catalysts for water oxidation could be enhanced by increasing the population of Co<sup>4+</sup> species present in the oxide.<sup>17,18,46,55–57</sup> It has been postulated that the Co<sup>4+</sup> species improve the electrophilicity of the adsorbed O, which is likely to promote the formation of O–OH via nucleophilic attack by an OH<sup>−</sup> anion with an O atom associated with Co<sup>4+</sup> species.<sup>18,57</sup> The enhancement in catalytic water oxidation activity on TiO<sub>2</sub> overcoated Co/C catalyst may be related to the role of TiO<sub>2</sub> in facilitating the oxidation of surface Co oxide. From these



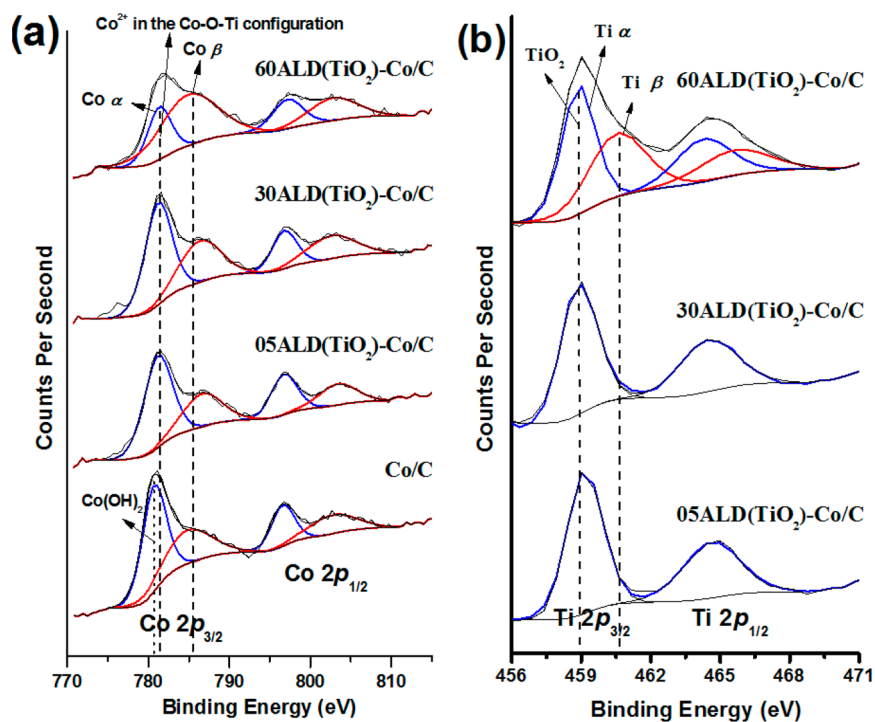


**Figure 4.** XPS analysis of the prepared ALD(TiO<sub>2</sub>)-Co/C catalysts. X-ray photoelectron spectra of (a) Co(2p) and (b) Ti(2p) for the ALD(TiO<sub>2</sub>)-Co/C catalysts.

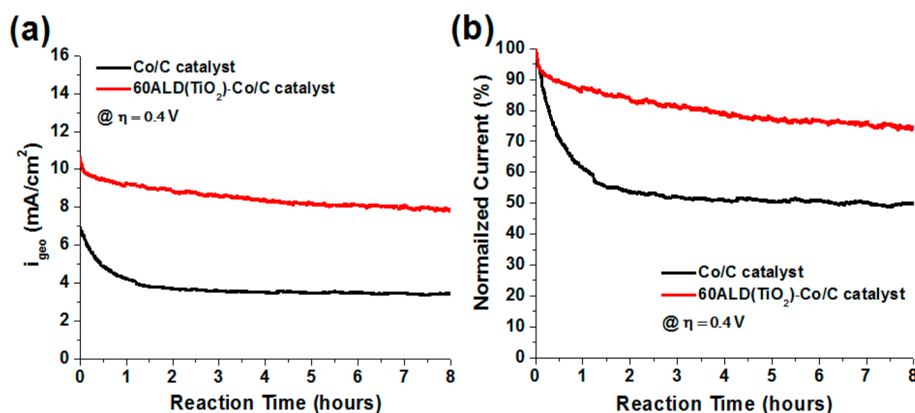


**Figure 5.** Stability tests of Co/C and 60 cycle ALD(TiO<sub>2</sub>)-Co/C for electrocatalytic water oxidation at room temperature and in an aqueous 1 M KOH solution. (a) chronoamperometry measurements ( $i_{\text{geo}}$  vs time plot) and (b) chronoamperometric responses (% of current retained vs time plot) using rotating disk electrode (rotation speed: 1600 rpm) at  $\eta = 0.4$  V for 8 h.

XPS results and the observation of kinetic parameters, we hypothesize that the TiO<sub>2</sub> overcoating on Co/C catalyst changes the nature of the active sites, thereby promoting the formation of O–OH (known as the rate-limiting step for the reaction) more effectively, which could improve the water oxidation activity. In Figure 4b, the BE (458.9 eV) of Ti 2p<sub>3/2</sub> peak in the ALD(TiO<sub>2</sub>)-Co/C catalysts is attributed to TiO<sub>2</sub>.<sup>51,58</sup> Only in the 60 cycle ALD(TiO<sub>2</sub>)-Co/C catalyst, the Ti 2p<sub>3/2</sub> peak has two components of Ti  $\alpha$  and Ti  $\beta$ . There is not much record of a Ti  $\beta$  peak at this high binding energy (460.5 eV) in the literature. It has been attributed to band bending caused by the metal–TiO<sub>2</sub> interface.<sup>59–61</sup>

To investigate catalyst stability during water oxidation, chronoamperometry measurements were performed using a rotating disk electrode (rotation speed: 1600 rpm) on the Co/C and 60 cycle ALD(TiO<sub>2</sub>)-Co/C catalysts at  $\eta = 0.4$  V for over 8 h. In Figure 5a, the steady-state  $i_{\text{geo}}$  of the 60 cycle

ALD(TiO<sub>2</sub>)-Co/C was found to be stable compared to that of the Co/C. Also, Figure 5b confirms that the stability of the 60 cycle ALD(TiO<sub>2</sub>)-Co/C catalyst was improved (only ~25% activity loss after 8 h) compared to the Co/C catalyst (~50% activity loss after 8 h). The TiO<sub>2</sub> overcoated Co/C catalyst had a lower deactivation rate than the uncoated Co/C catalyst. We conducted additional TEM characterizations to understand why the TiO<sub>2</sub> overcoated Co/C catalyst had a higher stability than the uncoated Co/C (see Figure S7). After the electrochemical stability test, the cobalt particle size of the Co/C increased from  $19.1 \pm 6.9$  nm to  $34.5 \pm 13.1$  nm. However, the cobalt particle size of the used 60ALD(TiO<sub>2</sub>)-Co/C ( $22.1 \pm 8.5$  nm) did not statistically change (fresh 60ALD(TiO<sub>2</sub>)-Co/C had a particle size of  $20.3 \pm 7.7$  nm). In addition, the cobalt loadings of Co/C and 60ALD(TiO<sub>2</sub>)-Co/C after the electrochemical stability test did not change compared to those of the fresh Co/C and 60ALD(TiO<sub>2</sub>)-Co/C (see Table S2). It has been also reported

that the Co nanoparticle catalysts are stable toward dissolution during electrolysis in alkaline solution.<sup>17</sup> This result suggests that the stability enhancement by ALD coating is due to preventing the catalyst from sintering rather than catalyst leaching in electrochemical water oxidation reaction. It has been observed that sintering or leaching of metal nanoparticles begins at under-coordinated metal atoms located at defects, corners, and edge sites.<sup>35,62</sup> Recently, we have reported that the thin TiO<sub>2</sub> overcoating probably decorates these under-coordinated cobalt sites located at defects, corners, and edges, which thereby prevents the sintering or leaching of cobalt.<sup>36</sup>

In summary, TiO<sub>2</sub>-coated Co/C catalysts prepared by ALD were used to study the effect of TiO<sub>2</sub> overcoating on Co/C catalysts for electrochemical water oxidation. The catalytic activity of the ALD(TiO<sub>2</sub>)-Co/C catalyst increased when the ALD(TiO<sub>2</sub>) coating cycle number increased from 5 to 60. The 60 cycle ALD(TiO<sub>2</sub>)-Co/C catalyst showed 2.5 times higher TOF than the commercial Pt/C catalyst. In addition, the 60 cycle ALD(TiO<sub>2</sub>)-Co/C was found to be highly stable compared to Co/C. This work shows how the ALD technique can be used to enhance catalytic activity and stability of nonprecious metal catalysts for electrochemical water oxidation. This study also paves the way for future catalyst design in electrochemical applications such as fuel cells and electrolyzers.

## ■ ASSOCIATED CONTENT

### Supporting Information

The Supporting Information is available free of charge on the ACS Publications website at DOI: 10.1021/acscatal.5b00173.

All experimental sections and additional figures (PDF)

## ■ AUTHOR INFORMATION

### Corresponding Author

\*E-mail: huber@engr.wisc.edu.

### Present Address

<sup>†</sup>(H.J.K.) Center for Carbon Resources Conversion, Korea Research Institute of Chemical Technology (KRICT), Daejeon, Republic of Korea

### Author Contributions

All authors have given approval to the final version of the manuscript.

### Notes

The authors declare no competing financial interest.

## ■ ACKNOWLEDGMENTS

This material is based upon work supported as part of the Institute for Atom-efficient Chemical Transformations (IACT), an Energy Frontier Research Center funded by the U.S. Department of Energy, Office of Basic Energy Sciences. The authors would like to acknowledge Dr. Rob McClain for the help with the RDE experiments. The authors gratefully acknowledge partial support of this research by NSF through the University of Wisconsin Materials Research Science and Engineering Center (DMR-1121288).

## ■ REFERENCES

- (1) Turner, J.; Sverdrup, G.; Mann, M. K.; Maness, P. C.; Kroposki, B.; Ghirardi, M.; Evans, R. J.; Blake, D. *Int. J. Energy Res.* **2008**, *32*, 379–407.
- (2) Holladay, J. D.; Hu, J.; King, D. L.; Wang, Y. *Catal. Today* **2009**, *139*, 244–260.

- (3) Spurgeon, J. M.; Lewis, N. S. *Energy Environ. Sci.* **2011**, *4*, 2993–2998.
- (4) Huber, G. W.; Chheda, J. N.; Barrett, C. J.; Dumesic, J. A. *Science* **2005**, *308*, 1446–1450.
- (5) Vispute, T. P.; Zhang, H. Y.; Sanna, A.; Xiao, R.; Huber, G. W. *Science* **2010**, *330*, 1222–1227.
- (6) Prasomsri, T.; Nimmanwudipong, T.; Roman-Leshkov, Y. *Energy Environ. Sci.* **2013**, *6*, 1732–1738.
- (7) Lee, J.; Kim, Y. T.; Huber, G. W. *Green Chem.* **2014**, *16*, 708–718.
- (8) Jaouen, F.; Proietti, E.; Lefevre, M.; Chenitz, R.; Dodelet, J. P.; Wu, G.; Chung, H. T.; Johnston, C. M.; Zelenay, P. *Energy Environ. Sci.* **2011**, *4*, 114–130.
- (9) Durst, J.; Siebel, A.; Simon, C.; Hasche, F.; Herranz, J.; Gasteiger, H. A. *Energy Environ. Sci.* **2014**, *7*, 2255–2260.
- (10) Hunt, S. T.; Nimmanwudipong, T.; Roman-Leshkov, Y. *Angew. Chem., Int. Ed.* **2014**, *53*, 5131–5136.
- (11) Marcilly, C. J. *Catal.* **2003**, *216*, 47–62.
- (12) Zeng, K.; Zhang, D. *Prog. Energy Combust. Sci.* **2010**, *36*, 307–326.
- (13) Rossmeisl, J.; Qu, Z. W.; Zhu, H.; Kroes, G. J.; Nørskov, J. K. *J. Electroanal. Chem.* **2007**, *607*, 83–89.
- (14) Gorlin, Y.; Jaramillo, T. F. *J. Am. Chem. Soc.* **2010**, *132*, 13612–13614.
- (15) Esswein, A. J.; McMurdo, M. J.; Ross, P. N.; Bell, A. T.; Tilley, T. D. *J. Phys. Chem. C* **2009**, *113*, 15068–15072.
- (16) Hunter, B. M.; Blakemore, J. D.; Deimund, M.; Gray, H. B.; Winkler, J. R.; Müller, A. M. *J. Am. Chem. Soc.* **2014**, *136*, 13118–13121.
- (17) Chou, N. H.; Ross, P. N.; Bell, A. T.; Tilley, T. D. *ChemSusChem* **2011**, *4*, 1566–1569.
- (18) Yeo, B. S.; Bell, A. T. *J. Am. Chem. Soc.* **2011**, *133*, 5587–5593.
- (19) Liang, Y. Y.; Li, Y. G.; Wang, H. L.; Zhou, J. G.; Wang, J.; Regier, T.; Dai, H. J. *Nat. Mater.* **2011**, *10*, 780–786.
- (20) Garcia-Mota, M.; Bajdich, M.; Viswanathan, V.; Vojvodic, A.; Bell, A. T.; Nørskov, J. K. *J. Phys. Chem. C* **2012**, *116*, 21077–21082.
- (21) Louie, M. W.; Bell, A. T. *J. Am. Chem. Soc.* **2013**, *135*, 12329–12337.
- (22) McCrory, C. C. L.; Jung, S. H.; Peters, J. C.; Jaramillo, T. F. *J. Am. Chem. Soc.* **2013**, *135*, 16977–16987.
- (23) Ahn, H. S.; Tilley, T. D. *Adv. Funct. Mater.* **2013**, *23*, 227–233.
- (24) Mao, S.; Wen, Z. H.; Huang, T. Z.; Hou, Y.; Chen, J. H. *Energy Environ. Sci.* **2014**, *7*, 609–616.
- (25) Gao, M. R.; Sheng, W. C.; Zhuang, Z. B.; Fang, Q. R.; Gu, S.; Jiang, J.; Yan, Y. S. *J. Am. Chem. Soc.* **2014**, *136*, 7077–7084.
- (26) Deng, X.; Tüysüz, H. *ACS Catal.* **2014**, *4*, 3701–3714.
- (27) Surendranath, Y.; Kanan, M. W.; Nocera, D. G. *J. Am. Chem. Soc.* **2010**, *132*, 16501–16509.
- (28) Surendranath, Y.; Dincă, M.; Nocera, D. G. *J. Am. Chem. Soc.* **2009**, *131*, 2615–2620.
- (29) Kanan, M. W.; Nocera, D. G. *Science* **2008**, *321*, 1072–1075.
- (30) Blakemore, J. D.; Gray, H. B.; Winkler, J. R.; Müller, A. M. *ACS Catal.* **2013**, *3*, 2497–2500.
- (31) Grzelczak, M.; Zhang, J.; Pfrommer, J.; Hartmann, J.; Driess, M.; Antonietti, M.; Wang, X. *ACS Catal.* **2013**, *3*, 383–388.
- (32) Bachmann, J.; Zierold, R.; Chong, Y. T.; Hauert, R.; Sturm, C.; Schmidt-Grund, R.; Rheinlander, B.; Grundmann, M.; Gosele, U.; Nielsch, K. *Angew. Chem., Int. Ed.* **2008**, *47*, 6177–6179.
- (33) George, S. M. *Chem. Rev.* **2010**, *110*, 111–131.
- (34) Lu, J.; Fu, B.; Kung, M. C.; Xiao, G.; Elam, J. W.; Kung, H. H.; Stair, P. C. *Science* **2012**, *335*, 1205–1208.
- (35) O'Neill, B. J.; Jackson, D. H. K.; Crisci, A. J.; Farberow, C. A.; Shi, F.; Alba-Rubio, A. C.; Lu, J.; Dietrich, P. J.; Gu, X.; Marshall, C. L.; Stair, P. C.; Elam, J. W.; Miller, J. T.; Ribeiro, F. H.; Voyles, P. M.; Greeley, J.; Mavrikakis, M.; Scott, S. L.; Kuech, T. F.; Dumesic, J. A. *Angew. Chem., Int. Ed.* **2013**, *52*, 13808–13812.
- (36) Lee, J.; Jackson, D. H. K.; Li, T.; Winans, R. E.; Dumesic, J. A.; Kuech, T. F.; Huber, G. W. *Energy Environ. Sci.* **2014**, *7*, 1657–1660.

- (37) Alba-Rubio, A. C.; O'Neill, B. J.; Shi, F.; Akatay, C.; Canlas, C.; Li, T.; Winans, R.; Elam, J. W.; Stach, E. A.; Voyles, P. M.; Dumesic, J. A. *ACS Catal.* **2014**, *4*, 1554–1557.
- (38) O'Neill, B. J.; Jackson, D. H. K.; Lee, J.; Canlas, C.; Stair, P. C.; Marshall, C. L.; Elam, J. W.; Kuech, T. F.; Dumesic, J. A.; Huber, G. W. *ACS Catal.* **2015**, *5*, 1804–1825.
- (39) Chen, Y. W.; Prange, J. D.; Duehnen, S.; Park, Y.; Gunji, M.; Chidsey, C. E. D.; McIntyre, P. C. *Nat. Mater.* **2011**, *10*, 539–544.
- (40) Scheuermann, A. G.; Prange, J. D.; Gunji, M.; Chidsey, C. E. D.; McIntyre, P. C. *Energy Environ. Sci.* **2013**, *6*, 2487–2496.
- (41) Lichterman, M. F.; Shaner, M. R.; Handler, S. G.; Brunschwig, B. S.; Gray, H. B.; Lewis, N. S.; Spurgeon, J. M. *J. Phys. Chem. Lett.* **2013**, *4*, 4188–4191.
- (42) Hu, S.; Shaner, M. R.; Beardslee, J. A.; Lichterman, M.; Brunschwig, B. S.; Lewis, N. S. *Science* **2014**, *344*, 1005–1009.
- (43) Yang, J.; Walczak, K.; Anzenberg, E.; Toma, F. M.; Yuan, G.; Beeman, J.; Schwartzberg, A.; Lin, Y.; Hettick, M.; Javey, A.; Ager, J. W.; Yano, J.; Frei, H.; Sharp, I. D. *J. Am. Chem. Soc.* **2014**, *136*, 6191–6194.
- (44) Yang, Q.; Choi, H.; Dionysiou, D. D. *Appl. Catal., B* **2007**, *74*, 170–178.
- (45) Zhou, H. C.; Song, J. L.; Fan, H. L.; Zhang, B. B.; Yang, Y. Y.; Hu, J. Y.; Zhu, Q. G.; Han, B. X. *Green Chem.* **2014**, *16*, 3870–3875.
- (46) Palmas, S.; Ferrara, F.; Vacca, A.; Mascia, M.; Polcaro, A. M. *Electrochim. Acta* **2007**, *53*, 400–406.
- (47) Lyons, M. E. G.; Brandon, M. P. *J. Electroanal. Chem.* **2010**, *641*, 119–130.
- (48) Yang, J.; Liu, H.; Martens, W. N.; Frost, R. L. *J. Phys. Chem. C* **2010**, *114*, 111–119.
- (49) Biesinger, M. C.; Payne, B. P.; Grosvenor, A. P.; Lau, L. W. M.; Gerson, A. R.; Smart, R. S. C. *Appl. Surf. Sci.* **2011**, *257*, 2717–2730.
- (50) Lim, S. H.; Ferraris, C.; Schreyer, M.; Shih, K.; Leckie, J. O.; White, T. J. *J. Solid State Chem.* **2007**, *180*, 2905–2915.
- (51) O'Shea, V. A. D.; Galvan, M. C. A.; Prats, A. E. P.; Campos-Martin, J. M.; Fierro, J. L. G. *Chem. Commun.* **2011**, *47*, 7131–7133.
- (52) Rossmeis, J.; Logadottir, A.; Norskov, J. K. *Chem. Phys.* **2005**, *319*, 178–184.
- (53) Garcia-Mota, M.; Vojvodic, A.; Metiu, H.; Man, I. C.; Su, H. Y.; Rossmeis, J.; Norskov, J. K. *ChemCatChem* **2011**, *3*, 1607–1611.
- (54) Bajdich, M.; Garcia-Mota, M.; Vojvodic, A.; Norskov, J. K.; Bell, A. T. *J. Am. Chem. Soc.* **2013**, *135*, 13521–13530.
- (55) Casella, I. G.; Gatta, M. *J. Electroanal. Chem.* **2002**, *534*, 31–38.
- (56) Lyons, M. E. G.; Brandon, M. P. *Int. J. Electrochem. Sci.* **2008**, *3*, 1425–1462.
- (57) Gerken, J. B.; McAlpin, J. G.; Chen, J. Y. C.; Rigsby, M. L.; Casey, W. H.; Britt, R. D.; Stahl, S. S. *J. Am. Chem. Soc.* **2011**, *133*, 14431–14442.
- (58) Lewera, A.; Timperman, L.; Roguska, A.; Alonso-Vante, N. *J. Phys. Chem. C* **2011**, *115*, 20153–20159.
- (59) Abe, T.; Suzuki, E.; Nagoshi, K.; Miyashita, K.; Kaneko, M. *J. Phys. Chem. B* **1999**, *103*, 1119–1123.
- (60) Perkins, C. L.; Henderson, M. A.; McCready, D. E.; Herman, G. S. *J. Phys. Chem. B* **2001**, *105*, 595–596.
- (61) Abe, T.; Suzuki, E.; Nagoshi, K.; Miyashita, K.; Kaneko, M. *J. Phys. Chem. B* **2001**, *105*, 597–597.
- (62) Greeley, J. *Electrochim. Acta* **2010**, *55*, 5545–5550.